COBBLESTONE EFFECT ON SES

Tore Ulstein and Odd M. Faltinsen
Department of Marine Hydrodynamics
Norwegian University of Science and Technology
N-7034 Trondheim, Norway

SUMMARY

Wave induced vertical accelerations (cobblestone oscillations) of a SES in small sea states is studied. Resonant spatially uniform and nonuniform dynamic cushion variations are then important. A nonlinear time domain solution is used. The nonlinearities are mainly due to the flexible stern seal bag behaviour. It is demonstrated that both the spatially varying pressure underneath the flexible stern seal bag and the impact between the bag and the water are important for the vertical accelerations of the vessel. The influence of main parameters characterizing the stern seal bag is discussed.

1. INTRODUCTION

A problem with a Surface Effect Ship (SES) is high vertical accelerations in small sea states. This represents a comfort problem for passenger transportation. The phenomenon is often referred to as the cobblestone effect and is a resonance effect due to the compressibility of air in the air cushion. The cobblestone effect is excited because the water waves dynamically change the air cushion volume. The resonance phenomenon occurs at high frequencies relative to the resonance frequencies for the rigid body motions of displacement ships of similar length. The two lowest resonance frequencies in the air cushion of a 30-35 m long SES are approximately 2 Hz and 5-6 Hz. Due to the frequency of encounter effect there are waves with sufficient energy in small sea states that excite these resonance oscillations. The eigenfunction for the dynamic air cushion pressure is constant in space for the lowest eigenfrequency and represents acoustic wave resonances for the higher eigenfrequencies. [1] demonstrated the importance of the lowest eigenfrequency. [2], [3] and [4] showed that acoustic standing wave effects must also be included. [5] and [6] give simplified introductions to cobblestone oscillations. [2] documented by full scale measurements onboard a 35 m long SES the importance of the two lowest eigenfrequencis (see Fig. 1). Since the lowest eigenmode is constant in space, it affects mainly heave accelerations. The second eigenmode, which corresponds to the lowest acoustic resonance frequency, has a node approximately midships. It can be

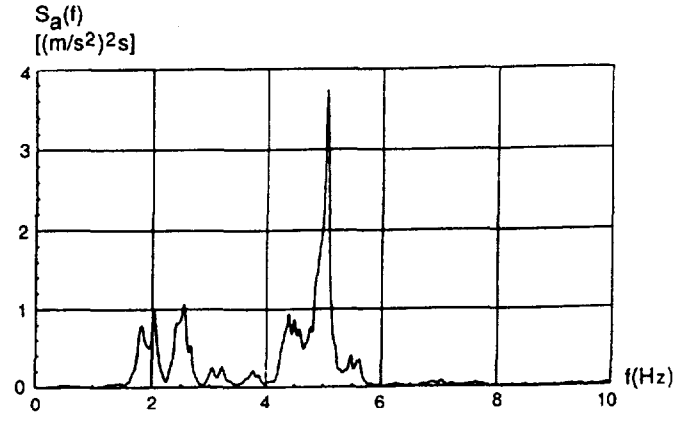

Fig. 1 Full scale measured spectrum $S_a(f)$ of vertical accelerations at bow of 35 m SES. Flexible stern seal bag. 45 knots. Head sea. $H_{1/3}$=0.3-0.4 m. f=frequency. Ref. [2].

approximated by a sinusoidal function. The modal wave length is roughly twice the ship length. It means that the second eigenmode affects mainly the pitch accelerations. Fig. 2 gives an overview over

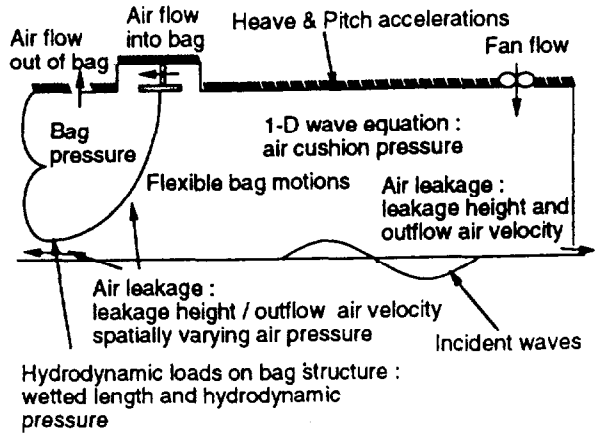

Fig. 2 Investigated physical effects.

investigated subproblems. Important damping mechanisms of the cobblestone oscillations are due to the air flow into the air cushion through the fans and the air leakage underneath the seals and through louvers

Paper presented at the RTO AVT Symposium on "Fluid Dynamics Problems of Vehicles Operating near or in the Air-Sea Interface", held in Amsterdam, The Netherlands, 5-8 October 1998, and published in RTO MP-15.

that are part of a ride control system. The placement of the louver system is essential. For instance if the louver system is placed midships, it will have a negligible effect on the acoustic resonance mentioned above. The reason is simply that the acoustic pressure component has a small amplitude midships, while it has its maximum absolute value at the ends of the cushion. Fig. 3 shows a proposed ride control system by [7]. A louver system consisting of two vent valves in the front

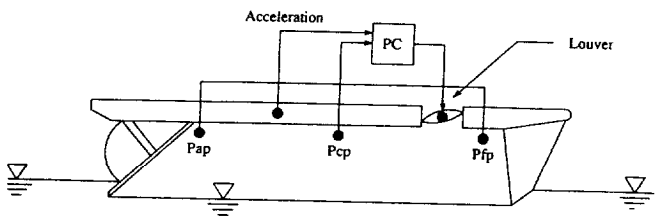

Fig. 3 Ride Control System. Ref. [7].

of the air cushion is used. The opening and closing of the vent valves control the air flow from the air cushion and cause damping of the cobblestone oscillations. Three pressure sensors were used in the air cushion and one accelerometer on the vessel as part of the ride control system. By properly filtering the signals from the measurement units and using a mathematical model for the behaviour of the SES, the control system can give the correct signals to the louver system. In order to construct a ride control system, a simplified but rational mathematical model is needed ([4]). This study focus on the nonlinear effects of the flexible stern seal bag. The cobblestone oscillations do not Froude scale. For instance resonance periods are approximately proportional to the ship length. This makes comparisons with model tests difficult. Full scale validation is needed.

2. THEORY

Head sea longcrested waves are assumed. A right-handed coordinate system that moves with the forward velocity U of the SES and is fixed to the mean oscillatory position of the vessel, is used. Here the X-axis points upstream in the direction of the forward velocity, and goes through the center of gravity (CG). The Y-axis points to the port side and the Z-axis is upwards. Both goes through CG. The equations of coupled heave (η_3) and pitch (η_5) motions are formulated in the time domain as

$$(M+A_{33}^h)\ddot{\eta}_3+B_{33}^h\dot{\eta}_3+C_{33}^h\eta_3+A_{35}^h\ddot{\eta}_5 +B_{35}^h\dot{\eta}_5+C_{35}^h\eta_5=F_r^h(t)+F_3^{ac}(t) \quad (1)$$

$$(I_5+A_{55}^h)\ddot{\eta}_5+B_{55}^h\dot{\eta}_5+C_{55}^h\eta_5+A_{53}^h\ddot{\eta}_3 +B_{53}^h\dot{\eta}_3+C_{53}^h\eta_3 = F_5^h(t)+F_5^{ac}(t) \quad (2)$$

t is the time variable and dot stands for time derivative. M is the structural mass and I_5 is the structural mass moment of inertia around the Y-axis of the SES. A_{ij}^h, B_{ij}^h and C_{ij}^h are hydrodynamic infinite frequency added mass, damping and restoring coefficients of the two side-hulls. F_i^h is the linear hydrodynamic excitation force on the side-hulls and F_i^{ac} is the nonlinear force acting on the SES due to integrated unsteady excess pressure in the air cushion in direction i. The nonlinearity in F_i^{ac} is mainly caused by nonlinear effects related to the flexible stern seal bag. The hydrodynamic loads on the hull are expressed by strip theory ([8]) . This is not an important part of the cobblestone analysis.

2.1 Global Air Cushion Model

The air cushion is analyzed in two steps. First a global flow model is studied. The air cushion is then approximated as a box. Air flow through fans, air leakage and the velocities of the bounding surfaces are accounted for. The global flow is later connected to a detailed model around the bag. The global model describes the air flow by the wave equation

$$\frac{\partial^2\phi}{\partial t^2} - v_s^2\nabla^2\phi = 0 \quad (3)$$

Here ϕ is the velocity potential, v_s is the velocity of sound in air and ∇^2 is the Laplacian operator. The linear dynamic pressure $\hat{p}_c$ can be expressed as $-\rho\partial\phi/\partial t$. Boundary conditions have to be imposed. Formally we can write that $\partial\phi/\partial n$ is equal to the normal velocity $\vec{V}(\vec{x},t)\cdot\vec{n}$ on the surface Γ that encloses the air cushion volume. The normal vector $\vec{n}$ to Γ is positive out of the air cushion. Since it is sufficient to consider a one-dimensional flow in the longitudinal direction, the normal velocities at the stern and seal regions are averaged over the height of the air cushion. For instance at the stern of the air cushion there is a combined effect of the flow between the inside of the bag and the air cushion, the motions of the air bag, and the leakage below the air bag. The motions of the air bag have an important effect on the lowest acoustic spatially varying natural mode of the air cushion. The boundary condition at the free water surface follows from the kinematic free surface condition. Only incident waves are considered. The boundary condition at the rigid part of the wetdeck follows from the heave and pitch velocities. The normal velocity at the fan is expressed by the steady fan characteristics. The Finite Element Method has been used to solve the problem. Eq. (3) is combined with the boundary conditions and written as

$$\int_{V_c} N^T(\nabla^2\phi - \frac{1}{v_s^2}\frac{\partial^2\phi}{\partial t^2})dV_c \qquad (4)$$

$$-\int_{\Gamma} N^T(\frac{\partial\phi}{\partial n} - V(\vec{x},t)\cdot \boldsymbol{n})d\Gamma = 0$$

Here N^T is the transposed of the trial function matrix N. The first term in Eq. (4) is rewritten by Green's theorem as

$$\int_{V_c} N^T\nabla^2\phi dV_c = \int_{\Gamma} N^T\frac{\partial\phi}{\partial n}d\Gamma - \int_{V_c}\nabla N^T\cdot\nabla\phi dV_c \qquad (5)$$

The analyzed domain is broken down into N_{el} small 1-D elements in the longitudinal direction. It is assumed that $\phi(\xi,t)=N(\xi)\{\phi(t)\}$ where $\{\phi(t)\}$ is a vector containing the node point values of the velocity potential of the air flow. A linear variation is used over each element. [9] verified the numerical method by comparing with the Finite Difference Method and by using an analytical solution based on mode superposition.

2.2 Local Air Cushion Model at the Stern

It is now focused on the details at the stern bag seal. A 2-D problem is solved in the longitudinal plane of the SES. The pressure is assumed spatially constant inside the bag. This pressure can be related to the pressure in the air cushion by using continuity of mass flow in and out of the bag. The air inside the bag is assumed compressible and an adiabatic relationship is used between the pressure and the air density. The bag structure is modelled as a cable in the cross-sectional plane. In the static case the bag is not touching the water, but the leakage height underneath the bag is assumed to be initially zero in the time domain solution procedure. The aerodynamic pressure force acting on the bag is an order of magnitude larger than the gravity force. The dynamic contributions from gravity will appear as restoring terms and can be neglected compared to the tension terms. The bag structure is therefore modelled as a weightless but not massless cable. The studied bag geometry is a typical 2-loop bag configuration (see Fig. 4). The static bag geometry is

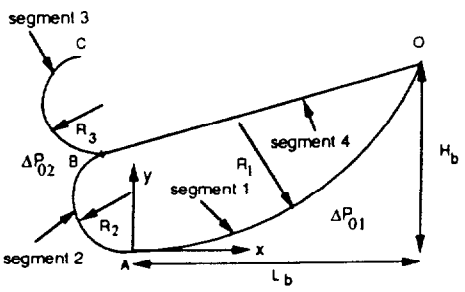

Fig. 4 Static geometry of 2-loop flexible bag seal.

approximated by 3 cable segments with constant radius of curvature R. This implies spatially uniform static difference pressure over each segment. The tensions in segments 1 and 2 are constant and equal. There are equal static difference pressures across segments 2 and 3, i.e., $\Delta P_{02}=\Delta P_{03}$.

The equations of motions for the flexible bag are derived by a linear perturbation of the static solution. Compatibility gives the relationship between tension and the motions in the transverse and the longitudinal directions. Since the radius of curvature R is constant for each cable segment, the equations of motions can be set up separately for each segment. Afterwards these cable segments are linked together with the boundary conditions. The equations of motions for a cable segment are finally written as

$$M_m\ddot{\eta}_n = T_0\frac{d^2\eta_n}{ds^2} + \frac{(T_0+EA)}{R}\frac{d\eta_t}{ds} - \frac{EA}{R^2}\eta_n + \Delta P_u \qquad (6)$$

$$M_m\ddot{\eta}_t = EA\frac{d^2\eta_t}{ds^2} - \frac{EA}{R}\frac{d\eta_n}{ds} \qquad (7)$$

Here η_n and η_t are the motions in the transverse and longitudinal directions. M_m is the structural mass per unit length of the cable. E is the elasticity modulus of the material. A is the cross dimensional area of unit width and T_0 is the static tension in the cable segment. s is the longitudinal coordinate along the cable segments (see Fig. 4) and ΔP_u is the unsteady difference pressure across the cable. The structural boundary value problem is solved by "dry" mode superposition. We can write

$$\eta_n(s,t) = \Sigma a_i(t)\phi_i^n(s) \qquad (8)$$

$$\eta_t(s,t) = \Sigma a_i(t)\phi_i^t(s) \qquad (9)$$

Here $a_i(t)$ is the principal coordinate of vibration mode number i and ϕ_i^n and ϕ_i^t are the mode shape functions in the transverse and longitudinal directions. A finite number of modes is used. Eqs. (8) and (9) are substituted into Eqs. (6) and (7). The two equations are multiplied with ϕ_j^n and ϕ_j^t, respectively and integrated over the length L_{cs} of all the cable segments. The two coupled equations of motions are added and give

$$M_{ji}\ddot{a}_i + C_{ji}a_i = \int_{L_{cs}}\Delta P_u\phi_j^n ds \qquad (10)$$

where

$$\int_{L_{cs}}\Delta P_u\phi_j^n ds = \int_{L_1}\hat{p}_{cal}\phi_j^n ds - \hat{p}_b\int_{L_1+L_2+L_3}\phi_j^n ds + \int_{L_1}p(s,\eta_n,t)\phi_j^n(s)ds \qquad (11)$$

Here $\hat{p}_b$ is unsteady pressure inside the bag. $p(s,\eta_n,t)$ is the unsteady hydrodynamic pressure. L_i is the length of bag segment number i. Since the hydrodynamic pressure is dependent on the bag deformations, the problem is hydroelastic. $\hat{p}_{cal}$ is the unsteady spatially varying air cushion pressure underneath the flexible stern seal bag. This is present when there is a gap between the lowest point of the bag and the free water surface.

We will show how $\hat{p}_{cal}$ and p are evaluated. We assume first the bag is not touching the water and p=0. A 2-D problem is analyzed. This information is used as a basis for a 1-D approximation. The flow is assumed quasi-steady and incompressible. The air is inviscid. Since the important wave lengths in the acoustic air cushion problem is much longer than the cross-sectional length dimensions of the air bag, the assumption of incompressibility is consistent from that point of view. However, when the air gap becomes very small, the local Mach number is high. The assumption of quasi-steady flow and inviscid air may also then be questioned. Since viscous effects are neglected, the separation point of the air flow must be chosen. The lowest point of the bag is used. The geometry and the coordinate system are defined in Fig. 5. Origo is placed at the steady free water surface. The x-axis is parallel to the undisturbed free water surface and is pointing towards the stern of the SES. The y-axis is pointing upwards. The velocity potential ϕ of the local air flow satisfies the 2-D Laplace equation. The kinematic condition on the free air surface is

$$\phi_y(x,y)=\phi_x(x,y)\zeta_x(x) \quad \text{on} \quad y=\zeta(x) \qquad (12)$$

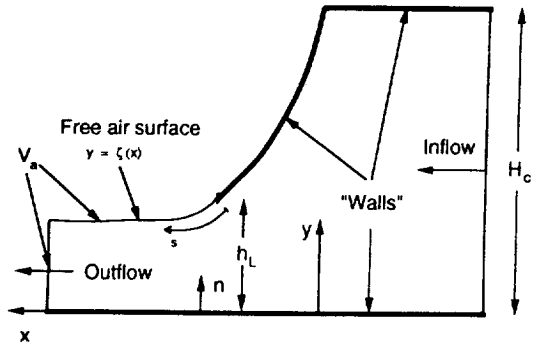

Fig. 5 Air flow underneath stern seal bag.

Here $\zeta(x)$ is the air surface coordinate defined in Fig. 5. The subscripts x and y denoted the x- and y-derivatives. The dynamic condition states that the pressure on the free air surface is equal to the atmospheric pressure. This implies that

$$\phi_s(x,y)=V_a \quad \text{on} \quad y=\zeta(x) \qquad (13)$$

The subscript s denotes the tangential derivative at the free air surface and V_a is the constant air flow velocity at the free air surface as indicated in Fig. 5. There are no normal velocity on the "walls". A Kutta condition is prescribed at the separation point (lip). It expresses that the tangential velocity and aerodynamic pressure are continuous at the lip. The horizontal uniform inflow velocity is assumed known and constant over the height of the air cushion. The outflow velocity V_a is assumed constant through the air jet. The velocity potential ϕ for the incompressible air flow inside the fluid domain is represented by Green's second identity, i.e.

$$2\pi\phi(\vec{x}_1)=\int_{S(\vec{x})}\left[Q(\vec{x},\vec{x}_1)\frac{\partial\phi(\vec{x})}{\partial n(\vec{x})}-\phi(\vec{x})\frac{\partial Q(\vec{x},\vec{x}_1)}{\partial n(\vec{x})}\right]dS(\vec{x}) \qquad (14)$$

Here S is the surface that encloses the air flow volume. The normal vector $\vec{n}$ to S is positive into the air flow domain. Further $Q=\log|\vec{x}_1-\vec{x}|$. When the field point approaches a point on the boundary, an integral equation of Fredholm type is obtained. The geometry is discretized into straight elements. The velocity potential and the normal velocity are assumed constant over each element. A set of linear equations follows from the discretization. To get a correct representation of the velocity potential on the lip of the bag, the equation that satisfies no normal velocity on the last element on the lip is exchanged with an equation that prescribes atmospheric pressure at the trailing edge. This implies that the tangential velocity at the separation point must be equal to V_a (see Eq. (13)). To establish this equation the local behaviour of the tangential velocity of the air flow near the lip is used. The unknowns are the normal derivative of the velocity potential on the free air surface and the velocity potential on the inflow and the wall surfaces. The solution procedure is as follows. First a jet contraction coefficient $k_a=\zeta(x\to\infty)/h_L$ (see Fig. 5) is guessed. A free air surface is generated based on this guess. This surface is described by an exponential function in the first iteration. The unknown coefficients in this function are determined from the approximation of the jet contraction coefficient and the fact that the tangent to the free air surface is equal to the tangent of the bag at the lip. An outflow velocity can be found from the jet contraction coefficient by mass conservation. The potential on the free air surface can now be found from the dynamic free surface condition defined in Eq. (13), since now both the velocity potential at the outflow surface and the tangential velocity at the free air surface are known. Green's second identity can then be used to find the normal derivative of the velocity potential on the free air surface. When this velocity is known, the

kinematic free surface condition is used to generate a new free air surface (see below), and the procedure is repeated until there is no updating of the free air surface or that the error estimate obtained from the conservation of momentum is below a chosen value (e.g. 1%). One important point is how the kinematic free surface condition is rewritten into an iterative scheme to update the free air surface. To obtain a stable and accurate solution, the kinematic free surface condition defined in Eq. (12) is rewritten into the following iterative scheme

$$\zeta_x^{N_{it}+1}=\frac{\zeta_x^{N_{it}}\phi_s^{N_{it}}+\phi_n^{N_{it}}}{\phi_s^{N_{it}}-\zeta_x^{N_{it}}\phi_n^{N_{it}}} \qquad (15)$$

It is used that $\zeta_x=-n_1/n_2$, $\phi_x=n_1\phi_n+n_2\phi_s$ and $\phi_y=n_2\phi_n-n_1\phi_s$. Here $\boldsymbol{n}=(n_1,n_2)$. The slope of the first element on the free air surface is set equal to the slope of the last element on the lip, and is not updated by the algorithm described above. The reason is the Kutta condition, that ensures a smooth flow at the separation point of the bag. Now both the velocity potential and its normal derivative are known on the whole enclosing surface. The air pressure is found from Bernoulli's equation. The method has been verified against analytical solutions based on conformal mapping ([9]). Since a more simplified method is beneficial in a ride control system, 1-D approximations have been studied. It has been found that the pressure distributions can be well described by

$$\frac{p(x)-p_a}{0.5\rho_a V_a^2}=1-(\frac{k_a h_L}{h(x)})^2 \qquad (16)$$

Here $h(x)$ is the local vertical distance between the water free surface and the bag. h_L is the value of h at the lowest point of the bag. The jet-contraction coefficient k_a is determined a priori by a 2-D analysis for a given bag. V_a is found by setting p equal to p_c upstream.

Water impact loads

The behaviour of a planing bag bouncing on the free water surface is analyzed as a water entry problem, assuming a large forward speed of the SES relative to the relative vertical velocity between the bag structure and the water surface. Gravity can be neglected. The wetted length of the bag will vary strongly through the impact on the free water surface. The hydrodynamic loading will be much larger than the aerodynamic loading due to the relatively low pressure in the air cushion and inside the bag. This implies that the immersion of the bag is low. The body boundary conditions can therefore be transferred to a straight horizontal line. This together with the free surface conditions leads to a square root singularity in the hydrodynamic pressure at the spray root in the planing problem. The modal hydrodynamic force defined by the last integral on the right hand side of Eq. (11), will not be affected by the detailed behaviour of the flow around the spray. The vertical global motions of the bag and the effect of the vertical motions due to incident waves are considered. A right-handed local xy-coordinate system that moves with the forward speed U of the vessel is used. The origin is fixed at the lowest point of the static bag configuration. The x-axis is positive towards the upstream direction of the undisturbed water flow and the y-axis is positive upwards. The undisturbed free stream velocity U is in the negative x-direction relative to this coordinate system. Since potential flow is assumed, the separation point must be determined a priori. The lowest point of the bag is chosen. The body boundary conditions are transferred to a straight horizontal line that corresponds to the x-axis (y=0) defined above (see Fig. 6). The total

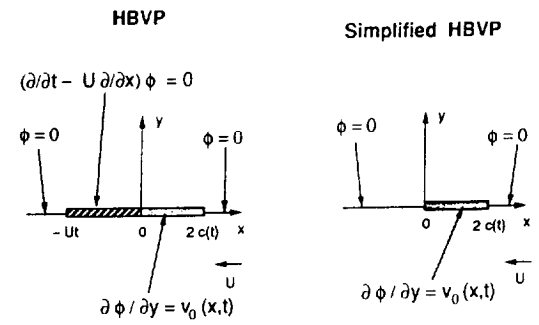

Fig. 6 Hydrodynamic boundary value problems (HBVP) for water entry of bag.

velocity potential is defined as $\Phi(x,y,t)=-Ux+\phi_I(x,y,t)+\phi(x,y,t)$ where $\phi_I(x,y,t)$ is the incident irregular wave potential and $\phi(x,y,t)$ is the velocity potential for the water flow caused by the bag. ϕ is found by a quasi-steady approach in the simplified Hydrodynamic Boundary Value Problem (HBVP). The dynamic free surface condition is approximated by ϕ=0 on $x<0$ and $x>2c(t)$. Here $2c(t)$ is the wetted length. At the wetted surface of the bag the following vertical velocity is prescribed

$$v_0(x,t)=\dot{\eta}_3+\frac{L}{2}\dot{\eta}_5+\frac{\partial\eta_{bag}}{\partial t}-U\frac{\partial\eta_{bag}}{\partial x}-\frac{\partial\phi_I}{\partial y} \qquad (17)$$

Here η_{bag} describes the unsteady geometry of the bag, that is the vertical distance between a point on the bag and a horizontal line defined by y=0. An approximation of the wetted length is found from

$$h_{L0}+\eta_{bag}(2c(t),t)=\zeta(-\frac{L}{2},t)-\eta_3(t)-\frac{L}{2}\eta_5(t) \qquad (18)$$

Here h_{L0} is the vertical distance between the lowest point of the bag and the free water surface at t=0 and ζ defines the incident wave profile. L is the length of the air cushion and the flexible bag is located at X=-L/2. Pile-up of water is neglected. A more correct way to define the HBVP is shown in Fig. 6. [10] and [11] solved this HBVP and did also include pile-up of water upstream the wetted part of the bag. This represents a more complicated procedure. Numerical studies by [9] showed that the errors using the simplified solution are not important.

3. RESULTS

Unsteady air cushion pressures and vertical accelerations of a SES are studied at AP, CG and FP. Here AP is located at X=-L/2, CG at X=0 and FP at X=L/2. The SES is described in Table 1. Head sea longcrested waves are assumed. A modified Pierson Moskowitch wave spectrum with peak period T_p=1.8 s is used. This spectral period is realistic for small sea states. The peak period is chosen so that there are significant vertical accelerations in the frequency domain around the first spatial pressure resonance of the air cushion. There is negligible wave energy at the lowest eigenfrequency. The results are organized so that the simplest simulation model is presented first. Different effects are then added, so the importance of each effect can be quantified. The results are presented in terms of response spectra as a function of frequency of encounter.

Table 1. Main particulars of SES

Weight (M)	140 000 kg
Air cushion length (L)	28 m
Air cushion height (H_c)	2 m
Air cushion beam (B_c)	8 m
Mean side-hull beam	1.5 m
Mean side-hull draft	1.0 m
Mean air cushion pressure (p_{c0})	510 mmWc
Mean fan flow rate (two fans) (Q_{i0})	2.8 m²/s
Linear air cushion fan slope (two fans) $(\frac{\partial Q}{\partial p})_0^c$	-0.00104 m²s/kg
Linear bag fan slope (two fans) $(\frac{\partial Q}{\partial p})_0^c$	-0.00063 m²s/kg
Longitudinal position of fans (X_f)	12 m
Forward speed (U)	23 m/s

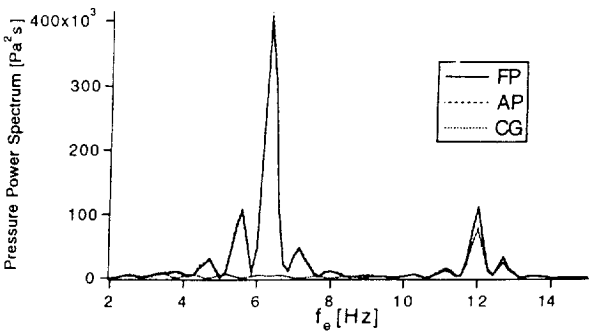

Fig. 7 Spectra of air cushion pressures. Air leakage neglected. Rigid stern seal. Head sea. T_p=1.8 s. $H_{1/3}$=0.15 m.

Fig. 7 shows the unsteady air cushion pressure when the stern seal is rigid and air leakage underneath the seals is neglected. The spectra have an oscillatory behaviour with many peaks. This is caused by amplification and cancellation effects in the volume pumping of the air cushion due to the incident waves. If the cancellation effect is disregarded, there are two main spectral peaks at approximately 6 and 12 Hz. These frequencies correspond to the two first spatial pressure resonances of a rectangular box, with length L=28 m. The spectral values around 6 Hz are nearly the same at AP and FP and nearly zero at CG. The reason is that the first eigenfunction for acoustic resonance in a rectangular box is equal to -1, 0 and 1 at AP, CG and FP. Around 12 Hz there is significant response also at CG. The reason is that the second eigenfunction for acoustic resonance is equal to -1, 1 and -1 at AP, CG and FP. Vertical accelerations at AP, CG and FP are presented in Fig. 8. The accelerations and the air cushion pressures have a similar behaviour, except that the accelerations around 12 Hz is negligible. Fig. 8 illustrates that the linear hydrodynamic wave excitation forces and moments on the side-hulls are negligible.

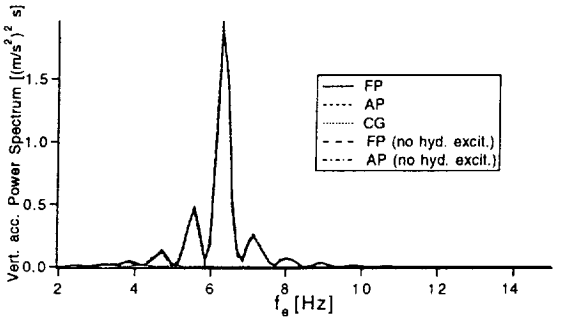

Fig. 8 Spectra of vertical accelerations. Air leakage neglected. Rigid stern seal. Head sea. T_p=1.8 s. $H_{1/3}$=0.15 m.

In order to illustrate possible deformation patterns of the stern seal bag, the static and the first four mode shapes of a 2-loop flexible stern seal bag are represented in Fig. 9. These mode shapes are the first four used (see Eqs. (8) and (9)) to describe the deformation of the flexible stern seal bag structure.

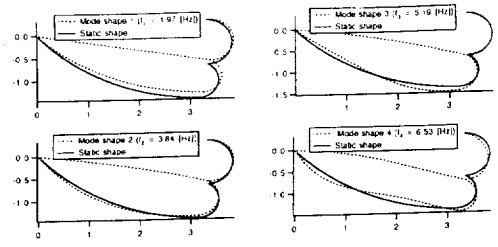

Fig. 9 Static configuration and first four mode shapes of flexible stern seal bag. Static difference pressures: ΔP_{01} = 500 Pa. ΔP_{02} = 5500 Pa. Bag length L_b=3.16m. Bag height H_b=1.4m. $EA=0.6\cdot 10^6$ N. M_m=4.3 kg/m.

Vertical accelerations at AP, CG and FP with a flexible stern seal bag are presented in Fig. 10. The air leakage underneath the seals is neglected. If Fig. 8 is compared with Fig. 10, some differences are observed. First one notes that the main spectral peak is shifted from approximately 6 Hz down to about 5 Hz. This is due to the flexible behaviour of the stern seal bag. The mechanism may be explained as follows; the flexible bag is deformed due to the unsteady air cushion pressure so that the deflected volume is in phase with the unsteady air cushion pressure. This leads to an equivalent horizontal velocity at the bag, due to the assumption of uniform pressure over the height of the air cushion. A simplified model can illustrate this phenomenon. Assuming harmonic time dependence $e^{i\omega_e t}$ and neglecting damping, the following eigenvalue problem can be defined

$$
\begin{aligned}
&-\omega_e^2\psi_{bsp}-v_s^2\,\psi_{bsp,x'x'}=0\\
&\psi_{bsp,x'}=0 \quad \text{at} \quad x'=0\\
&\psi_{bsp,x'}=\frac{dV_c}{dp_c}\frac{\rho_{c0}\omega_e^2\psi_{bsp}}{H_cB_c} \quad \text{at} \quad x'=L
\end{aligned}
\tag{19}
$$

Here i is the complex unit and $\psi_{bsp}e^{i\omega_e t}$ is the velocity potential of the air flow in the air cushion due to the motion of the bag. H_c and B_c are the cushion height and beam. ρ_{c0} is the steady mass density of air in the air cushion. dV_c/dp_c is a measure of the change in air cushion volume V_c due to bag deformation. It can be evaluated by noting that the right hand side of the boundary condition at $x'=L$ is a longitudinal velocity u' averaged over the cross-section of the air cushion. This can be expressed as

$$u'e^{i\omega_e t}H_cB_c=\frac{dV_c}{dt}=\frac{dV_c}{dp_c}\frac{dp_c}{dt}$$

Here $p_c=-\rho_{c0}i\omega_e\psi_{bsp}e^{i\omega_e t}$ is the dynamic pressure in the air cushion at $x'=L$. dV_c/dp_c can be estimated by a static analysis of the bag. The solution of the eigenvalue problem is $\psi_{bsp}=\bar{\psi}_{bsp}\cos rx'$ where $\omega_e=v_s r$ and

$$\tan rL+\frac{\gamma_s p_{c0}}{H_cB_cL}\frac{dV_c}{dp_c}rL=0 \tag{20}$$

Here r is the wave number of the standing pressure waves in the air cushion. Eq. (20) is the dispersion relation of the acoustic pressure waves inside the air cushion. When dV_c/dp_c is zero, $rL=\omega_e L/v_s=n\pi$, $n=1,2,\cdots$. This is a well known result for standing pressure waves in a long tube with rigid ends. Since $dV_c/dp_c>0$ for a flexible stern, the resonance frequency is reduced relative to rigid ends. The actual value depends on L,H_c,B_c, the ratio of specific heat of air γ_s and the steady excess pressure p_{c0} in the cushion.

Second one notes that the spectral peaks of the vertical accelerations at AP and FP in Fig. 10 are reduced with approximately 40% and 20% relative to Fig. 8. This reduction is explained by the flexible behaviour of the stern seal bag and the coupling between the bag pressure and the air cushion pressure at the bag. The differences between the vertical accelerations at AP and FP presented in Fig. 10, may be explained by the mode shape function of the pressure waves. If the previous simplified solution of ψ_{bsp} is used, then the variation in the longitudinal direction is given by $\cos rx'$. The ratio of ψ_{bsp} between AP and FP is $\cos rL$. Since rL is less than π, the absolute value of the ratio is less than 1. Fig. 10 shows that the flexible bag increases the accelerations in the region just above 10Hz. This increase is mainly explained by the volume change of the air cushion due to the deformation of the flexible stern seal bag.

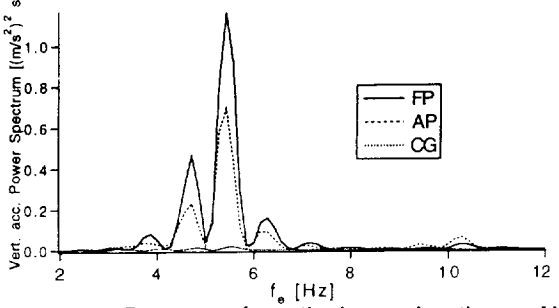

Fig. 10 Spectra of vertical accelerations. Air leakage neglected. Flexible stern seal bag. Head sea. T_p=1.8 s. $H_{1/3}$=0.15 m.

The effect of a constant leakage height underneath the stern seal bag can be studied by comparing Fig. 10 and 11. The vertical accelerations in Fig. 11 are decreased with approximately 10% relative to Fig. 10 around the first spatial pressure resonance frequency. The reason is additional damping caused by the air leakage underneath the stern seal bag.

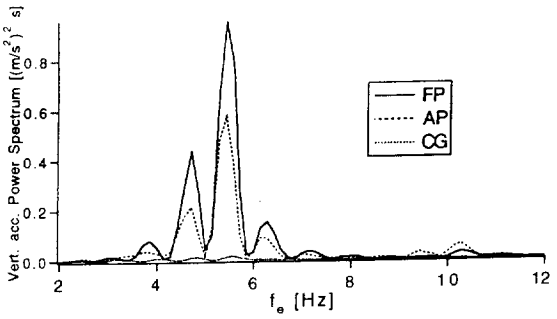

Fig. 11 Spectra of vertical accelerations. Constant leakage heights: 0 m (bow); 0.02 m (stern). Flexible stern seal bag. Head sea. T_p=1.8 s. $H_{1/3}$=0.15 m.

Vertical accelerations at AP, CG and FP accounting for variable leakage height underneath both the bow and stern seal are presented in Fig. 12. The variable leakage height underneath the seals is dependent on the relative motion between the seal and the water surface. The spatially varying pressure underneath the flexible bag is also accounted for. The static leakage height (h_{L0}) is set equal to -0.1 m and 0.02 m at the bow and the stern. The negative static leakage height at the bow means that the relative motion between the bow skirt and the water surface must be 0.1 m before air leakage at the bow occurs. These values of the static air leakage height are used through the remaining part of this section.

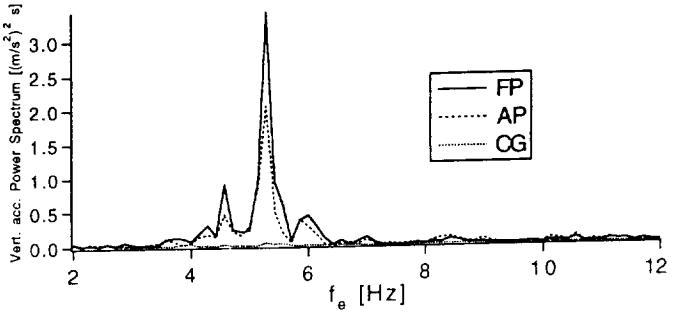

Fig. 12 Spectra of vertical accelerations. Variable air leakage. Spatially varying pressure underneath flexible stern seal. Head sea. T_p=1.8 s. $H_{1/3}$=0.15 m.

When vertical accelerations presented in Fig. 12 are compared with Fig. 11, one observes an increase of approximately 85% in the vertical accelerations around the first spatial pressure resonance frequency. An important reason is reduced damping due to smaller leakage height underneath the flexible stern seal bag. The spatially varying pressure underneath the bag forces the flexible bag to reduce the leakage height. There is also a change in the excitation of the air cushion pressure caused by the flexible bag motion.

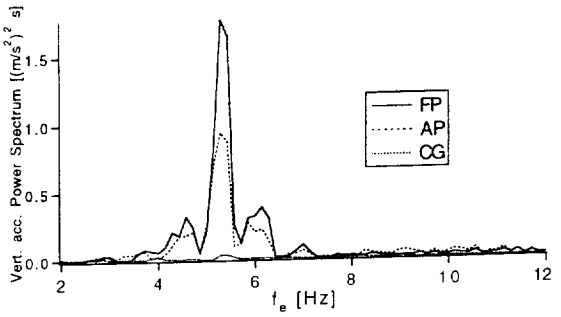

Fig. 13 Spectra of vertical accelerations. Variable air leakage. Spatially varying pressure underneath flexible stern seal. Water impact on bag. Head sea. T_p=1.8 s. $H_{1/3}$=0.1 m.

Vertical accelerations predicted by the complete model are presented in Fig. 13. The effect of air leakage underneath the seals is included together with hydrodynamic impact forces from the contact with the water. $H_{1/3}$ is reduced from 0.15 to 0.10 m in these calculations. This is necessary to avoid too large deformations of the bag structure and not contradict the assumption of a linear elastic model. These deformations are mainly caused by the interaction between the spatially varying pressure underneath the flexible bag and the hydrodynamic impact loads from the water. Since the bag structure is close to being horizontal in the impact region, a small increase in the immersion of the bag results in large increase in the wetted length. This causes large impact loads that punch the bag structure out of the water. On the other hand the spatially varying air pressure is in a way forcing the bag structure to reduce the leakage height underneath the bag. Many modes are needed to describe the dynamic behaviour of the bag during water impact. Improved convergence was achieved by introducing a bending stiffness term $-EI\partial^4\eta_n/\partial s^4$ on the right hand side of Eq. (6). The mode shapes corresponding to EI=0 were used. EI was set equal to 4.0 Nm^2. It was controlled that the global response was independent of this particular choice of EI as long as EI was small and larger than 3 Nm^2.

To evaluate the effect of the hydrodynamic impact between the flexible stern seal bag and the water, an analysis is made with the same model and data as described in Fig. 13, but without the effect of water impact. The results are presented in Fig. 14. The

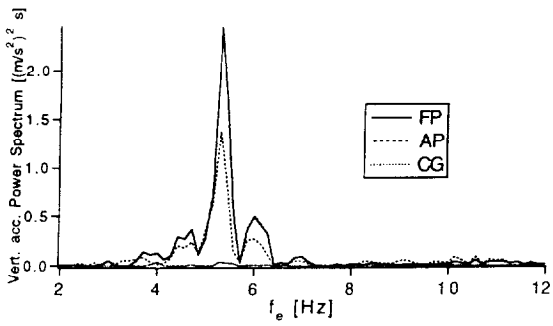

Fig. 14 Spectra of vertical accelerations. Variable air leakage. Spatially varying pressure underneath flexible stern seal bag. No water impact. Head sea. T_p=1.8 s. $H_{1/3}$=0.1 m.

largest differences between Figs. 13 and 14 occur in the frequency region around the first spatial pressure resonance of the air cushion (≈5 Hz). Spectral values for vertical accelerations are increased about 20% relative to the results in Fig. 13. One possible explanation is that the motion of the stern seal bag induced by the water impact affects the air cushion pressure similarly as a piston at the end of a long tube and may in this way cancel a part of the pressure variation in the air cushion. A probably more important reason is that the hydrodynamic impact punches the bag out of the water immediately after the initial impact so that an air leakage is recovered. The air leakage introduces damping and therefore reduces the vertical accelerations.

Since the results in Figs. 12 and 14 are obtained by the same physical model, but with different values of $H_{1/3}$, it illustrates that vertical accelerations are nonlinearly dependent on $H_{1/3}$. If the vertical accelerations had a linear behaviour, spectral value of the vertical accelerations at FP at the highest peak of the spectrum should be approximately 5.4 $(m/s^2)^2 s$ for $H_{1/3}$=0.15 m when the corresponding spectral value is 2.4 $(m/s^2)^2 s$ at $H_{1/3}$=0.10 m. Fig. 12 shows instead a value of 3.4 $(m/s^2)^2 s$ at $H_{1/3}$=0.15 m. This means that cobblestone oscillations of a SES can be overpredicted if linear transfer functions are used.

The airgap underneath the lowest point of the static bag configuration are presented as function of time in Fig. 15. The complete model is used. The significant difference between the two curves is due to the dynamic deformation of the lowest point of the bag. Fig. 15 illustrates that the flexible stern seal bag is "following" the water surface. A main reason is that the spatially varying pressures caused by the air leakage reduce the leakage. This behaviour is a characteristic feature of a flexible stern seal bag.

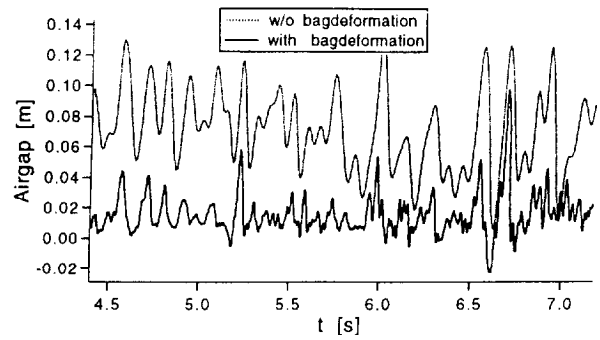

Fig. 15 Airgap underneath lowest point of static bag configuration as function of time. Effect of dynamic bag deformations. Full simulation model. (see also Fig. 13).

The previous analysis has in particular focused on the dynamics of the flexible stern seal bag and its effect on the vertical accelerations. An important parameter from a design point of view is the height to length ratio of the flexible stern seal bag. Fig. 16 shows vertical accelerations

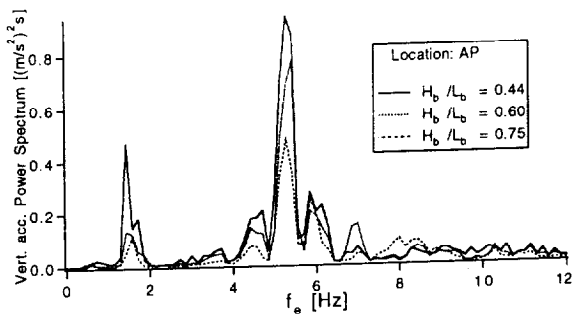

Fig. 16 Spectra of vertical accelerations at AP for different height to length ratios of flexible stern seal bag. Data and model as in Fig. 13.

at *AP* for three different height to length ratios of the flexible stern seal bag. When the height to length ratio is increased, the vertical accelerations are reduced. Similar results are obtained at FP. Fig. 16 shows also that the frequency region of the uniform pressure resonance is affected. The uniform pressure resonance frequency is approximately 1.6 Hz. Since the linear wave loads are negligible in this region due to the assumed wave spectrum, the response is due to nonlinear effects. One possible explanation for the reduced accelerations is that increased height to length

ratio of the flexible stern seal bag reduces the effect of the spatial pressure variation underneath the bag caused by the air leakage. This reduction may be explained as follows. The effect of the spatial pressure variation underneath the bag is mainly important in the region where the ratio between the leakage height and the height at the actual position is most influenced by the motion of the bag, that is the region near the lowest point of the bag. In the present case where the height to length ratio is increased, this implies that the length of this region is reduced and the effect of the spatial pressure variation as a result is reduced.

4. CONCLUSIONS

Cobblestone oscillations are theoretically studied in the time domain. Focus is on the influence of flexible stern seal bags and how the associated aero-hydroelastic problem can be simplified. It is shown by a case study that:

- The flexible stern seal bag reduces the lowest spatial resonance frequency of the air cushion. The elastic bag deformations are important for cobblestone oscillations.
- The spatially varying pressure caused by air leakage underneath the bag reduces the air leakage. This effect is important and increases the cobblestone oscillations.
- Hydrodynamic impact on the bag matters and reduces the vertical accelerations.
- Hydrodynamic wave induced loads on the side hulls are not important.
- Increased height to length ratio of the bag reduces the vertical accelerations.
- Vertical accelerations have a nonlinear dependence on significant wave height.

The analysis assumes that the incident waves pass undisturbed through the air cushion. The influence of the change in air cushion volume and leakage area due to diffraction of the incoming wave system by the presence of the side hulls, cushion pressure and bow seal should be studied. This includes interaction with the steady flow field. A quasi-steady analysis of the fans is used. [12] reports that dynamic fan effects may significantly reduce the spatially uniform pressure response in the air cushion.

Since the cobblestone oscillations are difficult to study in model scale [1], the theory needs to be validated by full scale results.

References

1. Kaplan, P., Bentson, J., Davis, S., "Dynamics and Hydrodynamics of Surface-Effect Ships", Trans. SNAME, Vol. 89, 1981, pp. 211-247.
2. Steen, S., "Cobblestone Effect on SES", Dr.ing. Thesis, Dept. Marine Hydrodynamics, Norw. Univ. of Science and Technology, Trondheim, Norway, 1993.
3. Steen, S., Faltinsen, O.M., "Cobblestone Oscillations of a SES with Flexible Bag aft Seal", J. Ship Res., Vol. 39, No.1, March 1995, pp. 25-41.
4. Sørensen, A.J., Steen, S., Faltinsen, O.M., "SES Dynamics in the Vertical Plane", Schiffstecknik, Bd 40, 1993, pp. 71-84.
5. Faltinsen, O.M., "Sea Loads on Ships and Offshore Structures", Cambridge University Press, 1990.
6. Faltinsen, O.M., "Hydrodynamics of High Speed Vehicles", Ch. 3 in Advances in Marine Hydrodynamics (Ed. M. Ohkusu), Computational Mechanics Publications, Southampton, Boston, 1996.
7. Sørensen, A.J., "Modelling and Control of SES Dynamics in the Vertical Plane", Dr.ing. Thesis, Dept. of Engineering Cybernetics, Norw. Univ. of Science and Techn., Trondheim, Norway, 1993.
8. Salvesen, N., Tuck, E.O., Faltinsen, O.M., "Ship Motions and Sea Loads", Trans. SNAME, Vol. 78, 1970, pp. 250-287.
9. Ulstein, T., "Nonlinear Effects of a Flexible Stern Seal Bag on Cobblestone Oscillations of a SES", Dr.ing. Thesis, Dept. Marine Hydrodynamics, Norw. Univ. of Science and Techn., Trondheim, Norway, 1995.
10. Ulstein, T., Faltinsen, O.M., "Hydroelastic Analysis of a Flexible Bag-Structure", 20th Symp. on Naval Hydrodynamics, University of California, Santa Barbara, USA, 1994.
11. Ulstein, T., Faltinsen. O.M., "Two-Dimensional Unsteady Planing", J. Ship Res., Vol. 40, No. 3, Sept. 1996, pp. 200-210.
12. Sullivan, P.A., Gosselin, F., Hinchey, M.J., "Dynamic Response of an Air Cushion Lift Fan", Proc. HPMV'92, Conference and Exhibits, ASME, Flagship Section, Arlington, VA, USA, 1992, pp. ACV39-ACV47.